Main Injector Upgrade R&D Collaboration on Electron Cloud Effects: Comparing the RF frequency of 53 MHz vs. 212 MHz*

M. A. Furman†
Center for Beam Physics
Lawrence Berkeley National Laboratory, Bldg. 71R0259
1 Cyclotron Rd.
Berkeley, CA 94720-8211
(Dated: March 18, 2008)

We compare, by means of simulations, the electron-cloud build-up for the Fermilab Main Injector (MI) for the present RF frequency $f_{\rm RF}=53$ MHz vs. a hypothetical RF frequency $f_{\rm RF}=212$ MHz at a given total beam population $N_{\rm tot}$. For simplicity, we assume the fill pattern for either RF frequency to consist of a single train of filled buckets followed by a single abort gap. We study the average electron-cloud density and incident electron-wall flux vs. $N_{\rm tot}$ in the range $N_{\rm tot}=(3.29-16.4)\times10^{13}$, for three assumed values of the peak secondary emission yield, namely $\delta_{\rm max}=1.2$, 1.3 and 1.4. The electron-cloud intensity shows a clear threshold behavior as a function of $N_{\rm tot}$: when $N_{\rm tot}$ exceeds a value $N_{\rm th}$, the average electron density rises strongly and roughly proportionally to $(N_{\rm tot}-N_{\rm th})$. The threshold $N_{\rm th}$ has a sensitive inverse dependence on $\delta_{\rm max}$. As expected, the simulated electron-cloud effect is weaker for the higher RF frequency: for a given $\delta_{\rm max}$, $N_{\rm th}$ is roughly a factor of 2 higher for $f_{\rm RF}=212$ MHz than for 53 MHz. If $N_{\rm tot}$ happens to lie above the threshold for $f_{\rm RF}=53$ MHz but below the threshold for 212 MHz, then the electron density in the latter case can be 4–5 orders of magnitude smaller than in the former. If $N_{\rm tot}$ is above the threshold for 212 MHz, then the electron density at this frequency is still lower than for 53 MHz, but only by a factor of a few.

I. ASSUMPTIONS.

For each $f_{\rm RF}$ we assume a fill pattern as follows:

$$f_{\rm RF}=53 \text{ MHz: } 548\times\text{F} + 40\times\text{E} \tag{1a}$$
$$f_{\rm RF}=212 \text{ MHz: } 2192\times\text{F} + 160\times\text{E} \tag{1b}$$

where "F" and "E" signify full and empty buckets, respectively.[1]

In any given fill pattern all the bunches have the same particle population N_b. When carrying out comparisons of the two frequencies, we assume that N_b for $f_{\rm RF}=212$ MHz is 1/4 that of the value for $f_{\rm RF}=53$ MHz, so that $N_{\rm tot}$ is the same in both cases. The range of values explored for $f_{\rm RF}=53$ MHz is $N_b=(6-30)\times10^{10}$, corresponding to $(1.5-7.5)\times10^{10}$ for $f_{\rm RF}=212$ MHz, and to $N_{\rm tot}=(3.29-16.4)\times10^{13}$ for either case. We look only at injection energy ($E_b=8.9$ GeV) and only at the location of the installed retarding-field analyzer (RFA). Concerning the RMS bunch length, we assume $\sigma_z=0.75$ m for $f_{\rm RF}=53$ MHz, and $\sigma_z=0.75/4=0.1875$ m for $f_{\rm RF}=212$ MHz. We assume that, at the RFA location, the pipe is round with radius $a=7.3$ cm and there is no magnetic field. We assume, for the purposes of parameter exploration, that the peak SEY $\delta_{\rm max}$ is in the range 1.2–1.4, which is the probable range for the actual MI chamber at the RFA location in its present state of conditioning [1, 2]. We use the stainless steel secondary emission model described in [3, 4], with the additional practical assumption that the SEY at 0 energy, $\delta(0)$, is proportional to $\delta_{\rm max}$.

When comparing the two RF frequencies, we only vary N_b and $\delta_{\rm max}$ while keeping $N_{\rm tot}$ fixed. For each case, we simulate one full MI revolution and compute the one-turn average electron-wall incident electron flux, electron-cloud density, and other related quantities (the electron-cloud density reaches steady state in a fraction, typically 10-20%, of a revolution period).

We use an integration time step $\Delta t=5\times10^{-11}$ s, a maximum of 20,000 macroelectrons allowed at any given time, and a 64×64 space-charge grid. Previous experience shows that, for the values of $\delta_{\rm max}$ considered here, these parameter values are adequate to reach numerical convergence. CPU running time on a Macintosh G5 (1.8 GHz) is 1.5–2.5 hrs for one full MI revolution, depending on $N_{\rm tot}$ and $\delta_{\rm max}$. Ideally, we would simulate the electron-cloud build-up and decay during the full MI ramp, lasting ~ 0.5 s of accelerator time. Given that the revolution period is ~ 11 μs, this would amount to $\sim$45,000 turns, clearly beyond present-day computer capabilities. Thus we only simulated the MI at injection energy, $E_b=8.9$ GeV.

Parameters of the physical model and the simulation method are summarized in Tables I and II, which also define various other symbols used in this note.

*Work supported by the FNAL MI Upgrade R&D Effort and by the US DOE under contract DE-AC02-05CH11231.
†Electronic address: `mafurman@lbl.gov`; URL: `http://mafurman.lbl.gov`

[1] The actual values of $f_{\rm RF}$ are 52.809 and 211.24 MHz.

TABLE I: Assumed MI fill pattern parameters for EC simulations.

Parameter	Symbol (unit)	Value	
RF frequency	$f_{\rm RF}$ (MHz)	52.809	211.24
Harmonic number	h	588	2352
No. of bunches	M	548	2192
Gap length	$\cdots$ (buckets)	40	160
Bunch spacing	$\cdots$ (buckets)	1	1
Bunch spacing	s_b (m)	5.645	1.411
Bunch spacing	t_b (ns)	18.94	4.734
Bunch population	N_b (10^{10})	$6-30$	$1.5-7.5$
RMS bunch length	σ_z (m)	0.75	0.1875
Total beam population	$N_{\rm tot}$ (10^{13})	$3.29-16.4$	

TABLE II: Other assumed MI parameters for EC simulations.

Parameter	Symbol (unit)	Value
Ring and beam parameters		
Ring circumference	C (m)	3319.419
Beam pipe cross section	$\cdots$	round
Beam pipe radius	a (cm)	7.3
Beam energy	E_b (GeV)	8.9
Relativistic beam factor	γ_b	9.486
Revolution period	T_0 (μs)	11.13
Bunch profile	$\cdots$	3D gaussian
Transverse RMS bunch sizes	(σ_x,σ_y) (mm)	(2.3,2.8)
Parameters for primary e$^-$ sources		
Residual gas pressure	P (nTorr)	20
Temperature	T (K)	305
Ionization cross-section	σ_i (Mbarns)	2
Ionization e$^-$ creation rate	n'_e ((e/p)/m)	1.266×10^{-7}
Secondary e$^-$ parameters		
Peak SEY	$\delta_{\rm max}\equiv\delta(E_{\rm max})$	$1.2-1.4$
Energy at peak SEY	$E_{\rm max}$ (eV)	292.6
SEY at 0 energy	$\delta(0)$	$0.29-0.34$
Simulation parameters		
Simulated section	$\cdots$	field-free region
Length of simulated region	L (m)	0.1
(Full bunch length)/(RMS bunch length)	L_b/σ_z	5
No. primary macroelectrons/bunch	$\cdots$	100
Max. no. of macroelectrons allowed	$\cdots$	20000
No. kicks/bunch ($f_{\rm RF}=53$ MHz)	N_k	253
No. kicks/bunch ($f_{\rm RF}=212$ MHz)	N_k	65
Integration time step	Δt (s)	5×10^{-11}
Space-charge grid	$\cdots$	64×64

II. RESULTS.

Fig. 1 shows the average incident electron flux J_e at the walls of the chamber (we checked that J_e on the RFA is essentially equal to the average of J_e over the entire chamber, despite the fact that the transverse beam shape is not round, but is rather upright with an aspect ratio $\sigma_x/\sigma_y = 2.3/2.8 \simeq 0.82$). For reference, the values of J_e in Fig. 1 might be compared with the measured RFA signal [5] for present-day fill patterns with $N_{\rm tot} \simeq (3{-}4)\times 10^{13}$: from the RFA calibration and estimated acceptance one infers an incident flux in the range $J_e \simeq (0-10)$ mA/m^2 [1, 2], with 5 mA/m^2 being a typical peak value usually obtained at $E_b \sim 60$ GeV.

Figure 2 shows the average electron-cloud density vs. $N_{\rm tot}$, along with the average beam neutralization density,

$$n_b = \frac{N_b}{\pi a^2 s_b} = \frac{N_{\rm tot}}{\pi a^2 s_b M} \tag{2}$$

For sufficiently high $\delta_{\rm max}$ and/or $N_{\rm tot}$, the average electron-cloud density exceeds the beam neutralization level. This condition is a very rough indication of the onset of single-bunch instability or emittance growth. A more direct indicator is the neutralization density within the 1-σ beam ellipse, which is much higher than the average value.

Figures 1 and 2 clearly exhibit a threshold behavior in $N_{\rm tot}$. When $N_{\rm tot}$ exceeds a certain value $N_{\rm th}$, the average electron-cloud density, to first approximation, grows like

$$n_e \simeq n_1(N_{\rm tot} - N_{\rm th}) \tag{3}$$

where $n_1 \simeq 0.04$ m^{-3}, roughly independently of $\delta_{\rm max}$ and $f_{\rm RF}$. On the other hand, as shown in Fig. 3, the threshold $N_{\rm th}$ does depend on both $\delta_{\rm max}$ and $f_{\rm RF}$, in the form

$$N_{\rm th} \simeq -N_1(\delta_{\rm max} - \delta_1) \tag{4}$$

where $N_1 \simeq 2.5 \times 10^{14}$, roughly independently of $f_{\rm RF}$, and

$$\delta_1 \simeq \begin{cases} 1.75, & f_{\rm RF} = 53 \text{ MHz} \\ 1.55, & f_{\rm RF} = 212 \text{ MHz} \end{cases} \tag{5}$$

The growth of n_e and J_e as a function of $N_{\rm tot}$ can be partially explained by the monotonic dependence of the electron-wall impact energy E_0 on $N_{\rm tot}$, as shown in Fig. 4. As E_0 increases towards the energy $E_{\rm max} \simeq 293$ eV where the SEY $\delta(E_0)$ has a peak, one naturally expects an increase in the effective SEY, hence a larger n_e. This argument, however, does not explain the above-mentioned threshold behavior, which probably involves a combination of secondary emission, space-charge forces, and the partial absorption of low-energy electrons striking the walls.

III. CONCLUSIONS.

The main results of our investigation are: (1) the electron-cloud intensity shows a clear threshold behavior as a function of $N_{\rm tot}$: when $N_{\rm tot}$ exceeds a value $N_{\rm th}$, the average electron-cloud density rises proportionally to $(N_{\rm tot}{-}N_{\rm th})$. (2) The threshold $N_{\rm th}$ has a sensitive inverse dependence on $\delta_{\rm max}$, and a sensitive direct dependence on $f_{\rm RF}$: for a given $\delta_{\rm max}$, $N_{\rm th}$ is roughly a factor of 2 higher for $f_{\rm RF} = 212$ MHz than for 53 MHz. For fixed $N_{\rm tot}$, this qualitative beneficial effect of the higher $f_{\rm RF}$ can be expected on rather simple grounds, because the correspondingly lower value of N_b makes the electron-wall impacts less energetic hence less effective in generating secondary electrons.

The dependence of $N_{\rm th}$ on $f_{\rm RF}$ affords the possibility of dramatically reducing the electron-cloud density assuming one has some freedom to chose the value of $N_{\rm tot}$. This is because there is always a range of $N_{\rm tot}$ for which the electron cloud is below threshold for $f_{\rm RF} = 212$ MHz but above threshold for $f_{\rm RF} = 53$ MHz. For example, in Fig. 2 (bottom) for the case $\delta_{\rm max} = 1.3$ and $N_{\rm tot} = 0.8 \times 10^{14}$, the simulated electron-cloud density n_e is almost 5 orders of magnitude smaller for $f_{\rm RF} = 212$ MHz than for 53 MHz. On the other hand, if $N_{\rm tot}$ is so high that it is above threshold for $f_{\rm RF} = 212$ MHz (and, *a fortiori*, for 53 MHZ), then the beneficial effect of the higher $f_{\rm RF}$ on the density is in the range of a factor of a few rather than several orders of magnitude.

Although the exercise carried out here is based on a simplified beam fill pattern, we expect the qualitative features of our results to remain valid for more complicated patterns, involving several gaps in the bunch train, provided the values of $N_{\rm tot}$ are in the range considered here.

This investigation does not address the effects of the electron cloud on the beam, which remain to be investigated separately.

Acknowledgments

I am indebted to I. Kourbanis and R. Zwaska for discussions, experimental results, and guidance.

---

[1] M. A. Furman, "Electron-Cloud Build-up in the FNAL Main Injector," LBNL-62738, June 4, 2007. Proc. Intl. Wkshp. on Electron-Cloud Effects "ECLOUD07" (Daegu, S. Korea, April 9-12, 2007),

http://chep.knu.ac.kr/electron cloud07/

[2] M. A. Furman, "Electron-Cloud Build-Up Simulations for the MI RFA: A Status Report," CBP-technote-387, 12 Nov. 2007, presented at the Project X Workshop, FNAL, 12-13 Nov., 2007. http://projectx.fnal.gov/Workshop/Index.htm

[3] M. A. Furman and M. T. F. Pivi, "Probabilistic model for the simulation of secondary electron emission," LBNL-49771/CBP Note-415 (Nov. 6, 2002). PRST-AB **5** 124404 (2003), http://prst-ab.aps.org/pdf/PRSTAB/v5/i12/e124404.

[4] M. A. Furman and M. T. F. Pivi, "Simulation of secondary electron emission based on a phenomenological probabilistic model," LBNL-52807/SLAC-PUB-9912 (June 2, 2003).

[5] I. Kourbanis, "e-Cloud MI Measurements", 26 Aug. 2007.

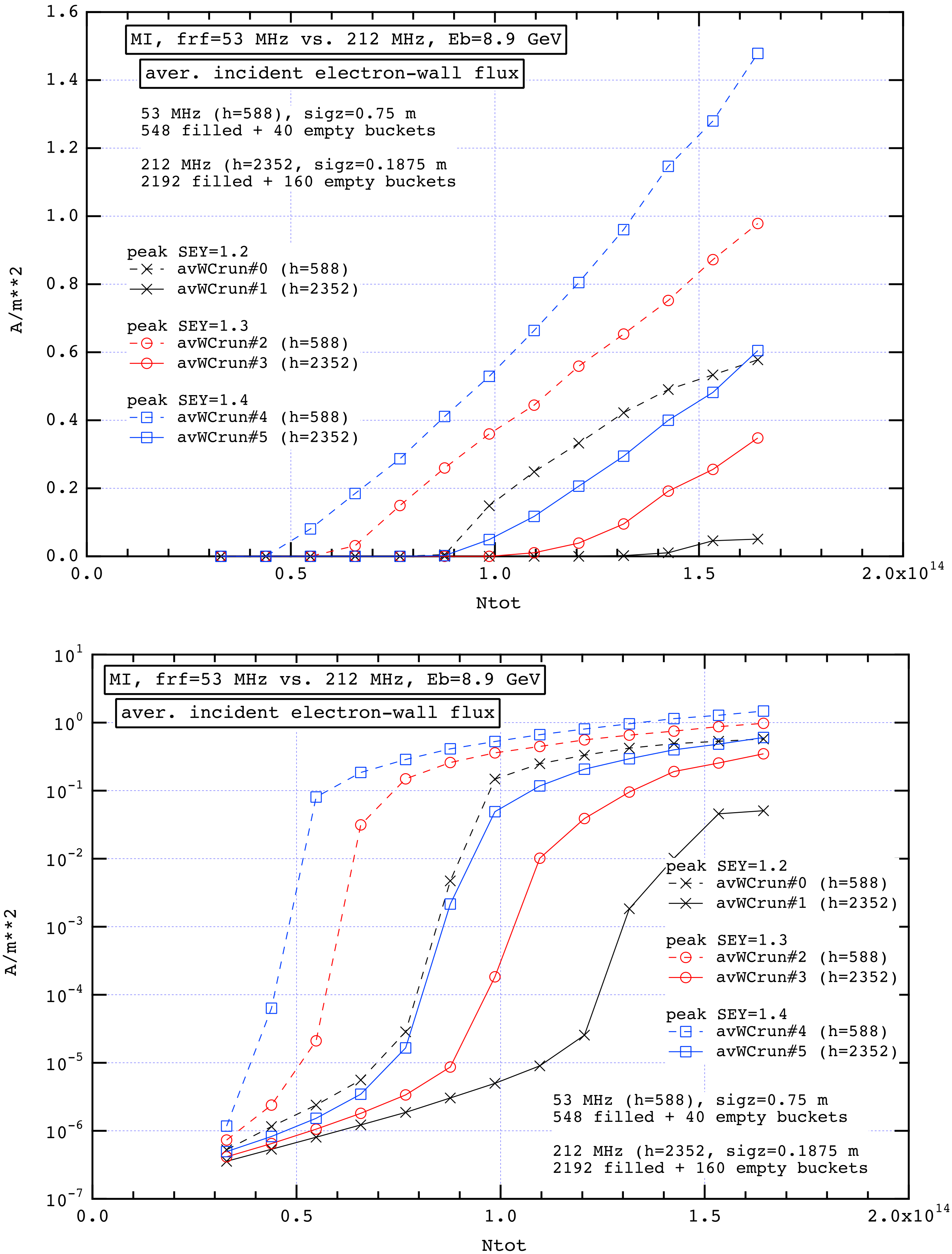

FIG. 1: Average simulated incident electron flux at the vacuum chamber walls. Top: linear scale; bottom: log scale (same data).

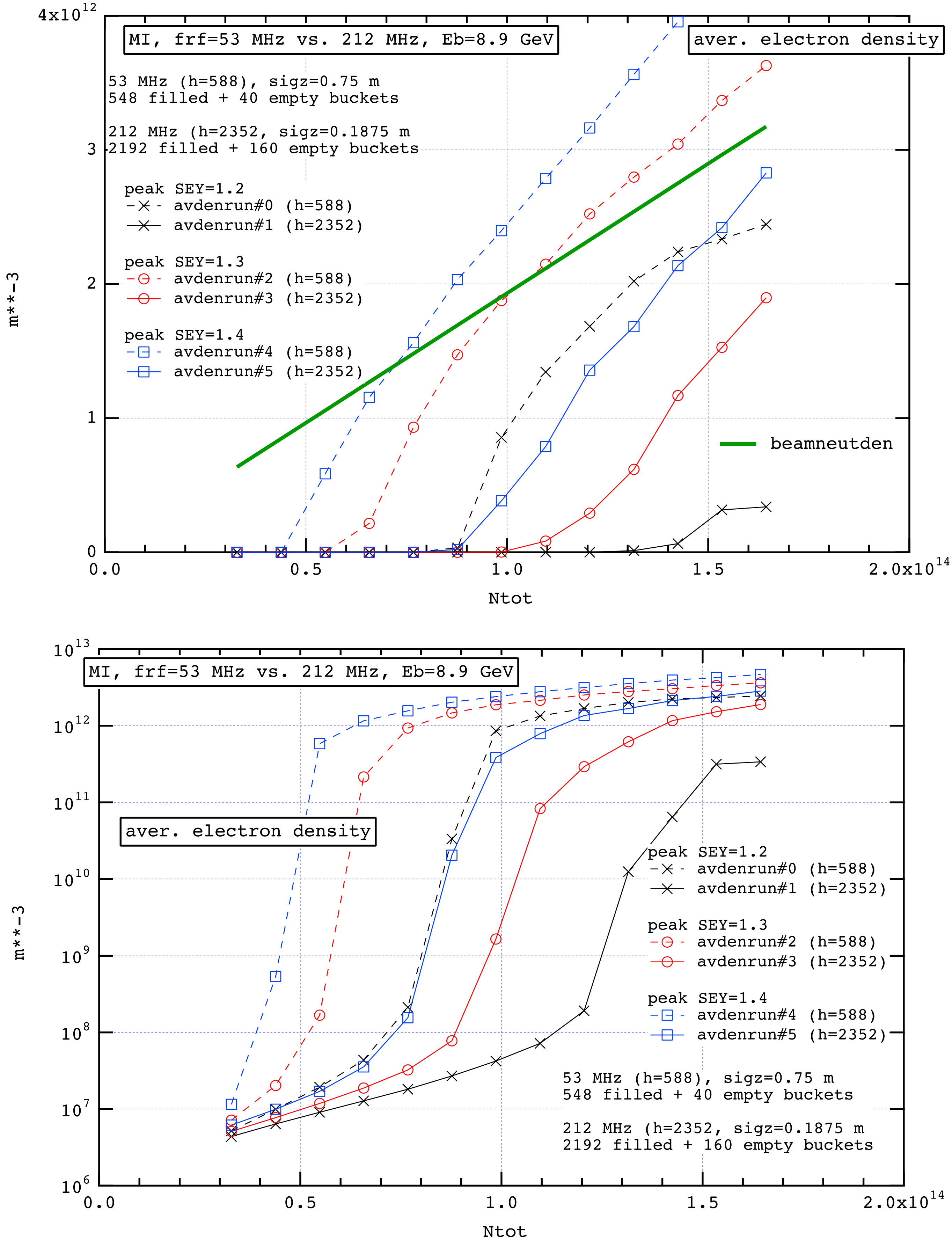

FIG. 2: Average simulated electron-cloud density. Top: linear scale; bottom: log scale (same data). The straight green line in the top plot is the average beam neutralization density, Eq. (2).

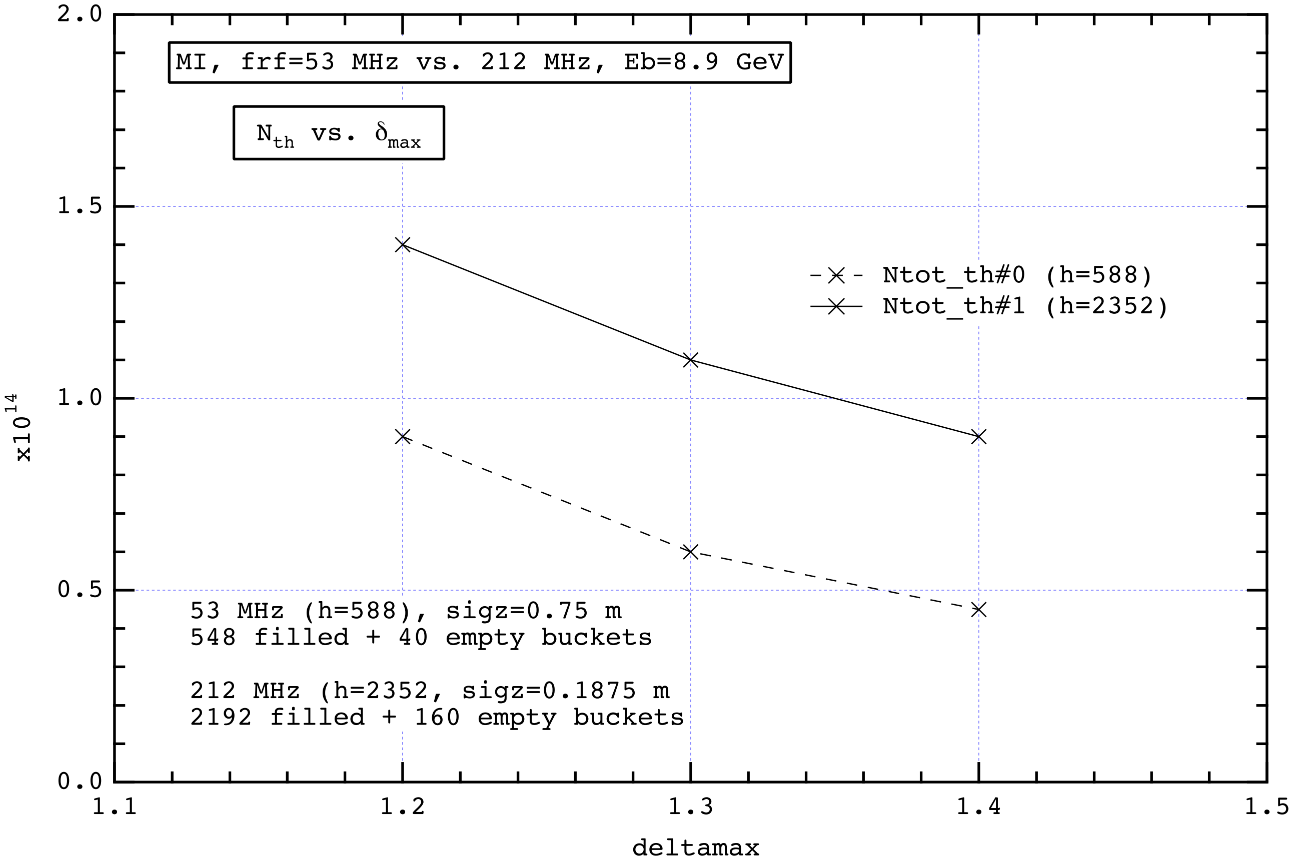

FIG. 3: $N_{\rm th}$ vs. $\delta_{\rm max}$ (Eqs. (4-5)).

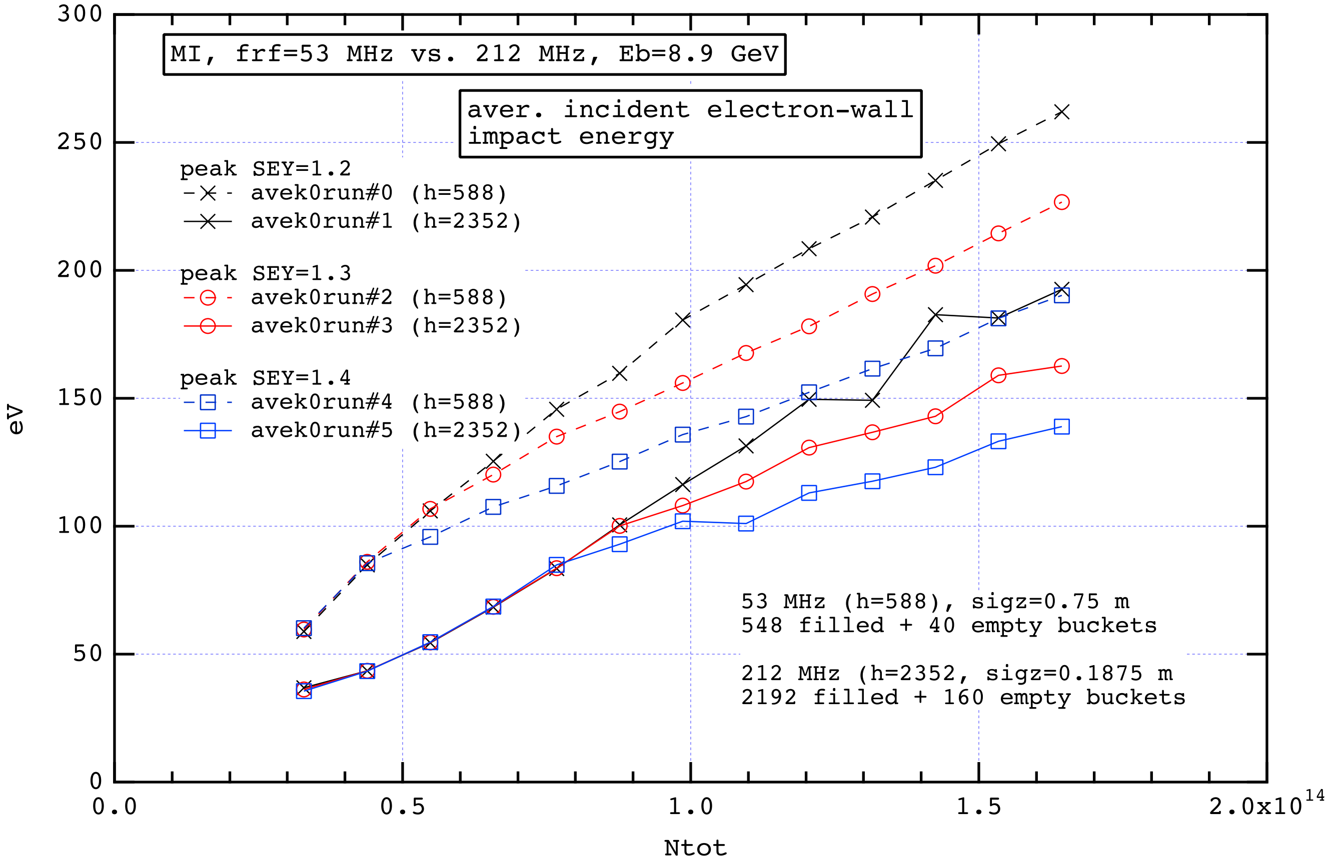

FIG. 4: Average simulated impact kinetic energy at the walls, per electron-wall collision.